Abstract

This document describes the development and implementation of a Pulsed laser deposition (PLD) based general tool for fast and efficient heterostructure device fabrication in the micrometer range, where the ability of the laser ablation process to generate quasi-stoichiometric vapor phase mass flow is leveraged with a sequential shadow mask scheme to allow multiple geometry-defining lithographic steps with several materials or experimental parameters in a single vacuum cycle.

1   Introduction

Current micro and nanofabrication processes rely on a surprisingly vast set of tools and technical capabilities, which implies a considerable capital expense. Small research organizations may acquire some of the tools required, but the fabrication process for standard devices require a substantial amount of steps which take enormous amounts of know-how and optimization procedures in order to perform with an acceptable rate of success. Even so, plenty of candidate materials currently researched for new technologies or improvement over existing capabilities require special, often complicated processing steps which are not trivially [combined] with the standard techniques of silicon-based devices, such as the coat-pattern-etch cycles required to generate a desired ...

1.1   Microfabrication

Photolithography + ebeam + soft lithography + ion beam as most used techniques in industrial and research contexts. Capabilities and shortcomings

This document first reviews some relevant characteristics, advantages and limitations of a set of techniques, namely multi-material PLD and the use of stencil lithography, which are combined in order to produce a flexible experimental thin film fabrication setup with capabilities which may be of interest to some workers in the broad material science field, as exemplified by a few selected use cases of the apparatus. Then the practical implementation is described, acknowledging current limitations and suggesting some natural improvements to realize the full potential of the proposed scheme.

2   Pulsed Laser Deposition

The design emerged as an upgrade for an existing PLD setup, used it a rather traditional [1] configuration. It uses a frequency doubled Nd:YAG in 3J, 30 ns boosts to ablate solid targets.

2.1   Technique Overview

As most physical vapor deposition technique, PLD relies on the generation of a vapor phase from the desired material which is collected in a substrate, generally perpendicular to the (average flow direction?)

A common deposition procedure consist on a cycle of many (relatively independent) repetitions of a conceptually simple process consisting on itself of a series of interrelated and partially overlapped steps [2]: Laser pulse, light absorption, target ablation, plume expansion and the eventual collision of the plume components with the substrate where collection of some species may ensue. Each of this steps is highly tunable by changing experimental parameters, an has particular effects on the final physical characteristics of the films or structures fabricated. [3]

2.2   Stoichiometry

As the light-material interactions occur in time scales substantially shorter than the thermal relaxation of the target, the ablation and plume formation processes take place away from thermodynamic equilibrium, and

thus the stoichiometric ratios of the materials present in the target are mostly conserved.[1]. This enables, at least in principle, the deposition of solids where some of the phases have very different partial pressures or bonding energy. Historically this has been the main advantage of the technique as compared with other PVD methods, driving it's use a research tool in areas where films of complex composition are critical, such as high Tc superconductors [5], oxide semiconductors [6] [7], exotic magnetic materials (such as antiferromagnetic [8], ferromagnetic insulators [9]), among many others.

2.3 Ease of energy Coupling

An often overlooked characteristic of PLD is how easy it is to control the timing, rate, amount and place where the energy is coupled onto the target to generate the desired ablation. This allow for sub-monolayer amounts to be easily deposited, and a quite dependable thickness control scheme. It also avoids to certain degree the need of active cooling within the chamber. The degree of control over the particular position where the laser impinges onto the target allows the implementation of several schemes to overcome some inherent limitations of the technique. See sections **??** y **??**

2.4 Mass Flow distribution

As the ablation process occurs within a localized region of the target, inducing a mass flow process which initiates in the surroundings of the irradiated region and that eventually evolves with certain characteristic divergence. The specifics of the plume shape and compositional spread depends heavily on the target's material, laser fluence / power and atmosphere characteristics, among others. In general the plume is much more 'forward directed' [10] [11] than in other PVD techniques, which on a static laser optical path severely limits the area where the deposits are relatively uniform. For example, lets consider the fabrication of X-Ray Bragg mirrors, which are fundamentally a periodic set of alternating uniform layers of different dielectrics traditionally fabricated by PVD methods. To avoid optical aberrations, such structures require a lateral thickness t gradient no grater than $\frac{\Delta t}{\Delta x} \leq 10^{-8}$ [12]. For a

However this issue is relatively easy to solve, and the low degree of divergence of the plasma plume helps avoid certain degree of the characteristics blurring effects of inherent of shadow mask.

Schemes to characterize a certain material mass distribution, use that information to generate a sequence of points for the laser to raster in order to deposit a even thickness over the whole substrate and a simple geometrical model to consider regarding blurring from multiple sources is presented in appendix ...

*** Practical Consideration
**** Vacuum Chamber and Geometrical Restrictions
****

3 Stencil Lithography

Stencil Lithography refers to the use of a usually solid mask with some defined apertures placed either in contact or some distance away from a substrate during a deposition process which effectively allows the spatially selective transfer of material. While this technique is seldom used in industry due to it's practical resolution limitations, the spatial modulation of mass flow through an aperture is an inherently clean process which imposes very few limitations on the nature of the deposited species, as opposed to conventional resist optical lithography, where etching processes need to be carefully tailored to avoid undesired interactions, specially when there are underlying layers with very different physicochemical characteristics. [13] It offers a series of benefits regarding reusability, ease of manipulation, avoidance of resist contamination, flexibility in regards to substrate

---

[1]There are plenty of reports, however, about a non stoichiometric component with a particular mass distribution profile found in targets with relatively high vapor pressure, usually attributed to evaporation due to local heating. See for example [4]
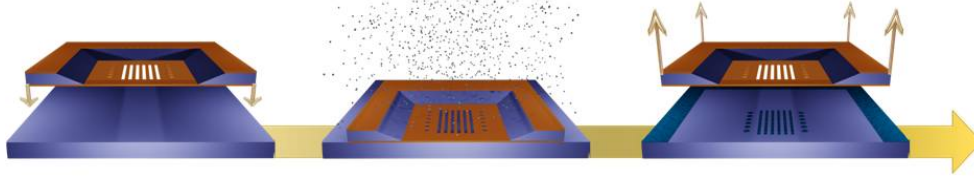
Figure 1:

characteristics and also allows the implementation of dynamic lithography schemes, where the pattern moves with respect to the substrate allowing a grater deal of flexibility and some unprecedented capabilities regarding spatially tailored thickness and compositional variations. It has been used in several experiments such as ...

3.1 Blurring Effects

A quite relevant issue regarding shadow masking has to do with the fact that the existence of a gap between mask ans substrate causes that any non collimated flow of material through the mask aperture generates a expanded version of the aperture. The effect has two main components: One regarding purely geometrical effects and another which is caused by adatom diffusion effects [14] [15]. Both components are clearly recognizable as they have quite different mass distribution profiles. For traditional PVD techniques, a simple geometrical analisis yields a geometrical blurring B_g given by:

$$B_g \simeq G\frac{D_{TM}}{D_{TS}} \tag{1}$$

where G is the mask-substrate Gap, D_{TM} the source materiel size and D_{TS} the distance between material and mask. The general idea extends

3.1.1 Geometrical Blurring

Cause

3.1.2 Adatom Diffusion and Mobility

Another component on stencil blurring has to do with the behaviour of the deposited particles

3.2 Stencil Clogging

As the material to be deposited flows through the mask apertures, some of the molecules stick to it's inner walls, effectively changing its geometrical profile. This effect may cause that a given structure becomes narrower as deposition advances, thus generation some sort of pyramidal shape. It also severely limits the reusability of the masks.

The effect becomes a relevant when the deposited thickness is in the same order of magnitude as the aperture size. The effect should be rather negligible for the intended aspect ratios and currently achievable aperture sizes (see section 5.3), and it may even be leverage to purposely generate smaller features or structures by intentionally narrowing the mask apertures.

3.3 Dynamic Shadow Masking

An interesting possibility which arises from keeping a distance between mask and substrate is the possibility of moving one with respect to the other during the deposition process, which allows transferring of patterns not

usually achievable with conventional stencils [2], the definition of regions on the same substrate with different composition and the fabrication of sectors with continuously varying thickness profiles among other things. Most existing configurations [16] [17] use some sort of in-vacuum manipulator to displace a static mask

3.4 Sequential Shadow Masking

The idea of using subsequent masking and deposition stages to fabricate multimaterial structures has already been described. In [17], Brugger et al. used a set of self aligned photoplastic stencils to perform multiple depositions changing the mask ex-situ. The mask had mechanical structures which helped to keep registration between structure to about $2\mu m$. In [18] and [19] multiple sequential masking steps (also ex-situ) were used to define spatially adressable

4 Multimaterial PLD + Sequential Shadow Masking: Use Cases

The combination of PLD and stencil lithography has already been used to fabricate structures of several relatively exotic materials such as perovskites [21] and the idea of sequentially While the present apparatus allows highly parallel fabrication, it's main intention is to serve as a quick prototyping tool which may lift some of the hurdles currently present in functional materials research, specially when considering small organizations or laboratories. The flexibility, speed and ease of use are specially convenient to generate proof-of-concept experiments and devices.

Figure 2: SEM images of a Si_3N_4 cantilever with FIB milled appertures to perform DSM

4.1 Multilayers

The availability of a set of different sources for ablation opens the possibility of fabricating a multilayer structures, which have a broad set of intrinsically interesting properties as well of technical applications such as optical coatings(which may used as filters or mirrors with finely tuned spectral response over broad regions of the EM spectrum) or .
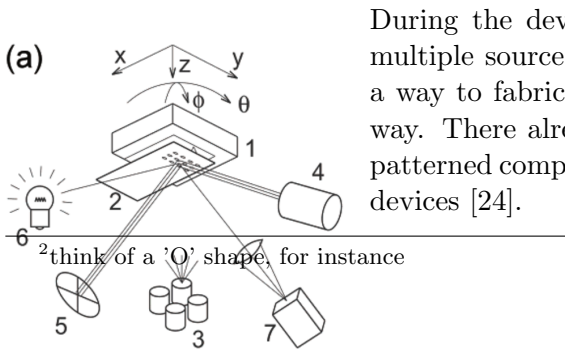
4.2 Heterostructures

During the development of this experimental configuration, the combination of multiple source materials with a set of sequential shadow masks was intended as a way to fabricate complex, multimaterial heterostructures in a relatively simple way. There already exist a series of reports of such kind of applications, such as patterned complex oxides [22], active devices [23], magnetic structures and photonic devices [24].

---

[2]think of a 'O' shape, for instance

Figure 3: DSM Multimaterial setup from [20]

The ability to almost arbitrarily pattern a region with a given material allows, at least in principle, the fabrication of a wide variety of devices such as junctions (pn, pin, Schottky barriers), volatile and non volatile memory elements (including ferromagnetic and ferroelectric elements, among other) thin film transistors, resistive elements, two terminal switches, light sources, photodetectors, electro-optic switches, waveguides, sensors and MEMS is relatively straightforward and opens up a vast array of pathways for fundamental and applied research. The justification behind this statement is that virtually any structure built by standard techniques is generated precisely by a sequence of such local compositional change, either by doping, deposition or selective etching. There are clear trade offs regarding resolution and perhaps some additional complexity in the mask designs. Furthermore, the ease of application of each subsequential feature may prove to be an interesting capability to inexpensively explore a wider variation on the integration architecture of several such devices. For example, 3D integration of circuit elements doesn't seem too far away from reach when the selective deposition of non active fillers may allow interconnection between several (hopefully epitaxial) layers. This of course comes with a substantial amount of challenges, but at least in principle the tool should be capable of generating such features.

4.3   Parallel Experiments, Compositional Spreads and Combinatorial Libraries

The development process of complex functional materials require navigating through a usually vast experimental variable space, where not only the particulars of the material composition are relevant, but also process parameters such as deposition conditions (substrate temperature, atmosphere, annealing steps, laser intensity). Even by using orthogonal experiments schemes the amount of samples needed to get an idea of how each of the variables influences the film or device characteristics and function may require several samples. A traditional set of sequential experiments not only has the problem of introducing random errors due to the non-concurrent nature of the fabrication process, but also may require unpractical amounts of capital and time.

Inspired by the pharmaceutical industry technique of combination synthesis for drug discovery and early experiments on phase-mapping [26], the approach of selectively and ... has become a effective and efficient method to generate an understanding of composition-structure-properties relations in unknown material systems.

Figure 4: Parallel experiment for the fabrication of oxide gas sensors. From [25]

Following [26], we may

Compositional spreads are films where some compositional parameters are continuou^{o}sly varied in some fashion, usually to study the local properties change in respect to such . It may be useful to probe critical composition surrounding phase transitions, or to optimize a given property such as dielectric strength, Band Gap energy [27],magnetoresistance [28], to name a few. Consider for example a chemical system such as the delaffosite system $CuFe_{1-x}Al_xO_2$.   One   may   be   interested   in   the   different
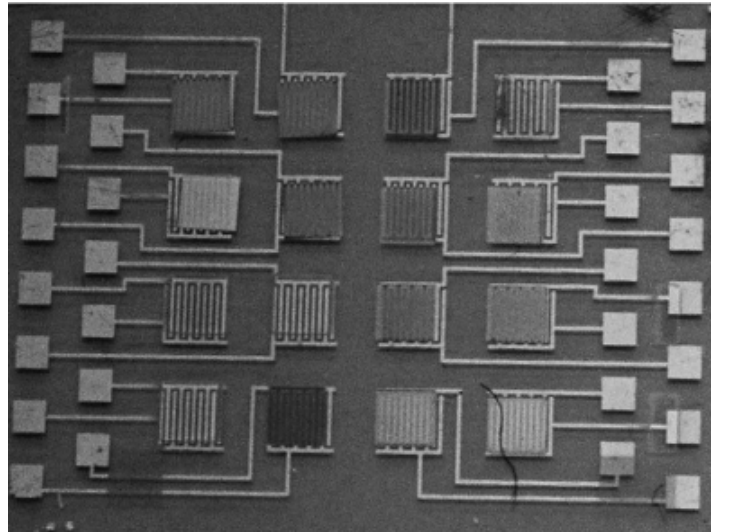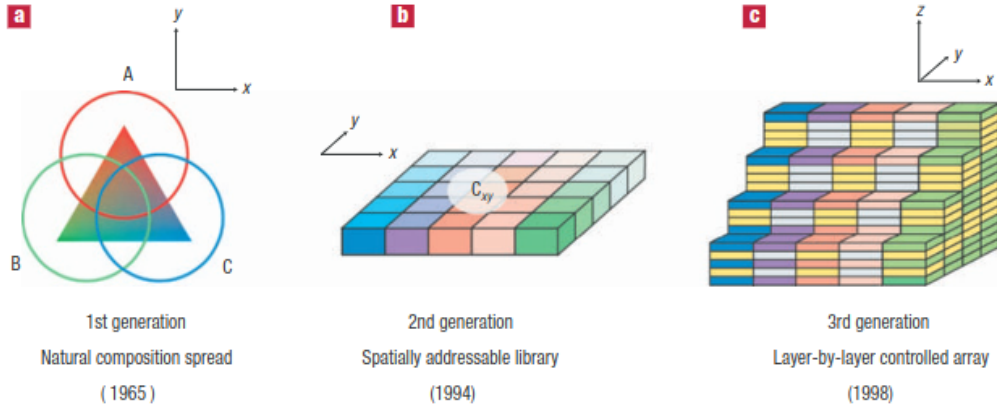
5

Figure 5: Some example of combinatorial or parallel schemes material synthesis. Figure shamelessly stolen from [26]
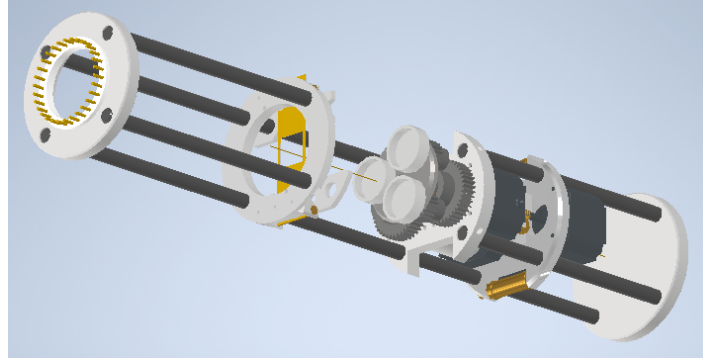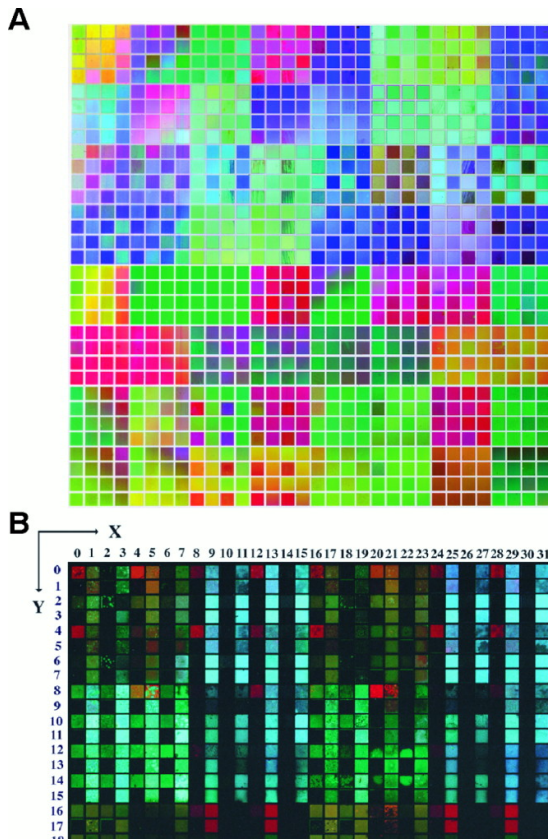

Figure 7:

5 Implementation

5.1 General Configuration

The design emerged while working with an existing vacuum chamber, which has a spherical configuration (ie the flanges main axis are radii of the sphere). A (??) inch flange with a (quick access hatch) was used to mount substrates and targets. This main flange is used as a sort of receptacle for a removable cylinder which contains most of the functionality. This fact that practically the whole system can be trivially taken out from vacuum allows for simpler operation and ease of use, but restricted the option of using standard manipulators for the actuation of the different mechanisms planned.
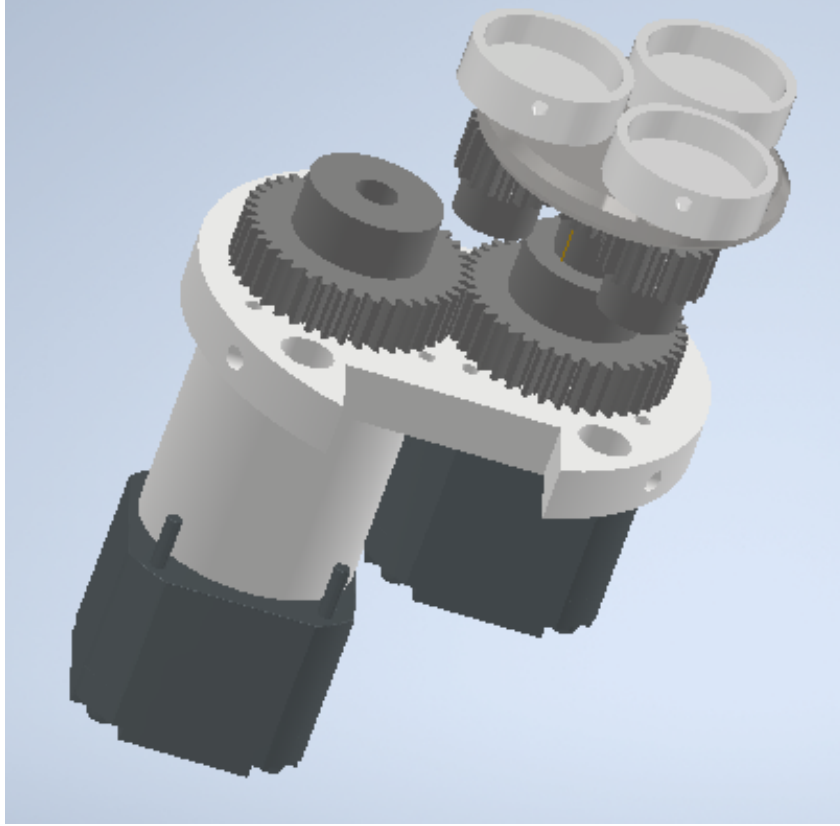
6

Figure 8: Multitarget carrousel

5.2   Multi-Target Carrousel

The mechanisms is directly based on a quite standard design, found in several publications and commercial instruments [29]. The two available degrees of freedom are actuated by a couple of vacuum compatible Nema 17 stepper motors with rigid shafts. The design allows the positioning of up to three 25 mm targets in the axis of the cylindrical capsule, while conforming to the overall radius restriction. The gears are standard and were bought from a online retailer. An etching process was performed to remove the black oxide coating that they presented, as I feared it might become a source of substantial outgassing. Most moving surfaces are lubricated by MoS_2 powder.

If for a given application there is need of more than three materials and keeping the whole process in controlled atmospheres is critical, it might be feasible to extend the amount of available materials by segmenting the target composition. This might require some timing considerations between the target rotation, pulse frequency and laser scanning cycle, but it does not impose any restrictions over film thickness homogeneity. See for example [30].
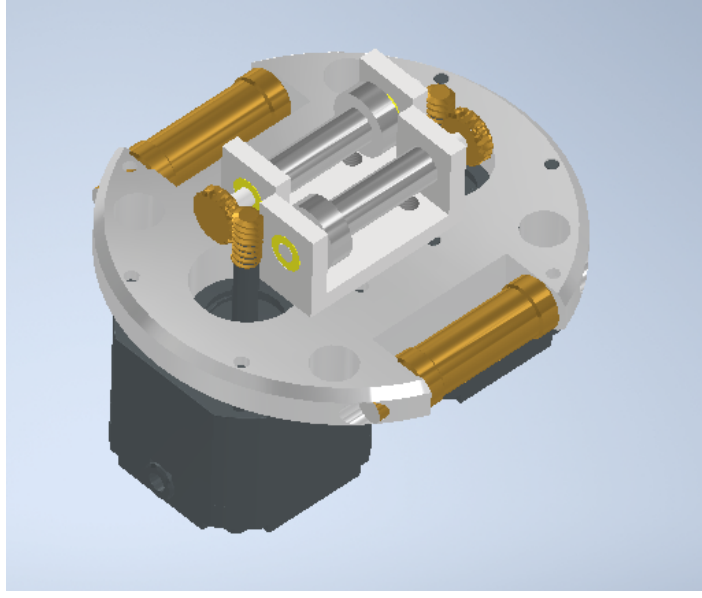
7

Figure 9: Tape Mechanism

5.3 Shadow Masks

As the masks need to deform substantially in order to be used sequentially due to space constraints, a 25 mm wide and 50 μm thick Polyimide tape is used as support for 50μm aluminum foil regions where the apertures are defined by means of laser micromachinig. Materials were chosen mainly due to availability, thermal resistance and the capabilities of the laser source used in the mask fabrication process. Indeed the polyimide low [modulus of elasticity?] is quite important to avoid deformations on the apertures due to tension and general manipulation.

An important concern that may naturally emerge is related to the possibility of a deformation of unsupported aluminum structures due to the convoluted path the tape has to follow. The main factor which may define the extent of this behavior is the ratio between the minimal radius of curvature of the path, which in the present case is about 3mm, and the characteristic dimension of the structure in the tape direction. This

[Empirical evidence on the relevance of the effect] A compromise between tensile strength and usable area was performed to define the masks size. 20mm a side squares constitute the effective area.

5.3.1 Fabrication

The mask fabrication process begins by outlaying the desired experiment(s) or device(s) intended, sketching the required depos itions steps, the nature of each (if its a static mask or a dynamic process) and how many masks are required for each deposition layer. Once the final mask count is clear, the blank tape es fabricated by means of a hobby-grade cutting plotter, which makes the required aluminum segment and the cutouts in the polyimide to expose the main region and the space for the alignment marks.

Then the mask are designed using the excellent open source software KLayout, which has plenty of capabilities helping the logical layout, among which the capability of generating custom cells by widely adopted programming languages is particularly interesting as it may help the eventual development of a collaboration ecosystem where such parametric designs can be shared. In fact such tools already exist in some niche application such as photonics.

Once ready, the blank tape is mounted on a homemade roll-to-roll system with tension control, individually controllable rollers and where a 1064 nm fiber laser engraver machines the required aperture. The engraver

8

manufacturer claims a 1 μm repeatability in the spot positioning over the whole 70X70 mm working area, but the smallest apertures achieved so far are in the 10 μm range.

5.4   Sequential Mask Mechanism

In order to expose the substrate to different masks, a mechanism consisting on two motorized rolls and a couple of guides was implemented. The Nema-17 vacuum compatible stepper motors are mounted parallel to the cylinder's main axis, and a worm gear mechanism is used to move the rollers in the appropriate direction while enhancing the positioning resolution. With the current roller size, each microstep represents a tape translation of about $0.8\mu m$ [3] The two motor design was chosen to allow some degree of tension control while allowing the tape to move in both direction, thus enhancing the flexibility of the deposition processes.

5.4.1   Mask Alignment Subsystem

As the mask fabrication is still quite artisanal, the mask's features may not be perfectly referenced to the tape's borders by as much as 1mm, which inhibits the possibility of registration by means of actuation alone due to placement repeatability concerns. Therefore, a scheme is devised where the masks are referenced a static set of registration marks, allowing at least in principle a placement accuracy to within the masks own resolution as the same fabrication process is used for both features and registration marks. While in research grade conventional lithographic processes the registration is checked by optical microscopy (and such schemes are indeed applied in apparatuses for in-vacuum registration [20] or reflective diffractometry [citation], in this case such arrangements are quite hard to implement, and thus a scheme where the degree of alignment between masks and the reference marks is measured by a light transmission scheme is implemented.

Placement of about 20 different masks with a registration in the order of a micrometer. Actual requirements may be dictated on the particulars of the devices / structures being fabricated.

5.4.2   Actuation

The aforementioned variation in mask fabrication implies that the range of actuator motion should be in the millimeter range, while ideally allowing? for displacements in the micrometer range. Due to space constraints, a compact actuation scheme is required, practically ruling out traditional motorization schemes. Thus, the options considered were both piezoelectric-stack based:either by a bridge/lever amplification compliant mechanism reach the required range, or by means of an inertial actuator inspired by the micromanipulator design described in [31], where the temporal profile of the signal fed to the stack defines whether a magnetically coupled translation stage moves along with the PZT or it slides with respect to the magnet, effectively expanding the range by several orders of magnitude. This approach was implemented due to a better compatibility to the machining capabilities available.

5.4.3   Positioning Feedback and Registration Marks

In order to ascertain the relative registration of the mask, a reference pattern is defined in the instrument structure (and thus is relatively static with respect to the substrate), while a matching pattern is cut onto the mask, at both sides of the stencil region.

A temporally modulated laser diode is shined through the reference marks to a photodiode. The signal on the photodiode is then a function of the relative alignment of the mask with respect to the reference patterns. Thus one may

---

[3]This quantity is inversely proportional to the rollers diameter, which effectively changes according to the amount of tape currently stored.

The accuracy of the overlay process is dependent of the minimal light intensity variation detectable by the photodiode in an (in principle very) noisy environment. Therefore, a signal acquisition scheme where phase-sensitive detection is implemented and fed to a variable gain self nulling amplifier

5.5 Laser Steering

As mentioned in section 2.4, the ablation process usually generates a relatively forward-directed plume, which translates in a quite relevant variation on the amount of deposited material as one moves through the substrate. Solutions for larger areas or more regular films are implemented either by scanning the substrate over the plume or the laser over the target, which is generally more technically feasible.

In this case a motorized kinematic mirror mount was implemented prior to the laser window to enable the capability of scanning the beam over the target. This not only enables the fabrication of larger regions of uniform thickness films, but is also critical to fabricate smaller structures through resolution enhancement techniques (app. 7.7) *** Actuator Design *** Mass Distribution Correction

5.6 Substrate Heater

A critical parameter when growing thin films is the substrate temperature, which heavily influence adatom dynamics and therefore film morphology and microstructure, both of

5.7 Process Control

6 Tests and Outline of a standard experimental procedure

7 Challenges and Prospects

7.1 A minimal subset of structures?

Is it possible to design a set of masks which combine in different ways in order to allow the creation of multiple devices as needed? Such scheme may be useful to avoid technological stagnation in situations where neither a complete microfabrication operation or a quick supply chain are available, such as space flight or in the early installation of planetary colonies. Just a though hehe

7.2 Beyond deposition

Deposition isn't the only technique used in semiconductor device fabrication. Spatially defined surface modification techniques such as etching (both kinetical and reactive), different functionalization processes and even ion implatation may in principle be integrated to this kind of configurations without much hassle.

7.3 Tension and parallelism control

7.4 Analog Harnesses

Recently some semiconductor foundries have allowed acces to die fabrication to the public, effectively sharing the required information and files needed to fine tune some standard IC layout tools to the particular capabilities of the foundry proccess. In some of the opportunities available to the public the individual designs are constrained to a region of the dye, while many of the interfacing functions are taking care by a 'harness' of devices, thus simplifying the requirement put on the hardware designer.
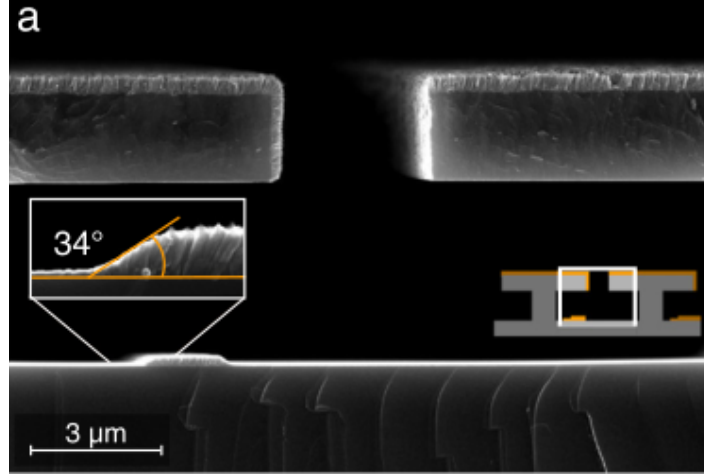
Figure 10: Evident displacement and (not so evident) blurring of a HV-CVD deposited feature with respect to the aperture which defined it

Such idea may as well be implemented in the context of device prototyping and characterization, where task such as signal conditioning, multiplexing and even some slight processing may be taken care on a predefined region of the substrate, thus allowing for simpler, faster and more efficient development progressions.

7.5 Particle control

7.6 Laser molecular beam expitaxy and In-situ characterization techniques

Another potentially useful characteristic of the ability to substantially move the mask relative to the substrate is that it allows its exposition to several in-situ characterization techniques that may require line-of-sight access to the film

7.7 Resolution Enhancement

The continuous drive towards miniaturization in commercial photolithographic processes ran in some point with feature's sizes which where beyond what could be practically resolved as per Rayleigh's criterion usi...

Mainly multi-patterning schemes -¿ Usually they require anysotropic etching

As discussed in the mass distribution section, the control of the laser spot placement in the targets surface with respect t a given aperture allows certain degree of control over the geometrical blurring component, and it also allows a certain amount of controlled displacement of the desired feature. Such effects have been reported and are well understood in the context of HV-CVD shadow masking [32] [22], where the flow of reactants usually comes from a set of nozzles which effectively acts as quasi-punctual Knudsen effusion cell. The apertures of the nozzles are both laterally displaced from the substrate center and also at an angle with respect to it's normal.

Therefore, as the precursor flow occurs in a pressure range where ballistic mass transfer predominates, one may use a rather simple geometrical model to describe such given displacement results in a displacement of the patterned feature. See appendix 8.1

The interesting bit in regards to the described setup is that the amount of displacement of the feature is basically a linear function of the distance between the material source and the aperture, scaled down by a factor which is of the order of $\frac{D_{ms}}{D_{tm}+D_{ms}}$, which can be easily in the order of 10^{-3} or even into the 10^{-4} range. Thus, with a placement accuracy of the laser spot placement in the order of a millimeter one already can generate
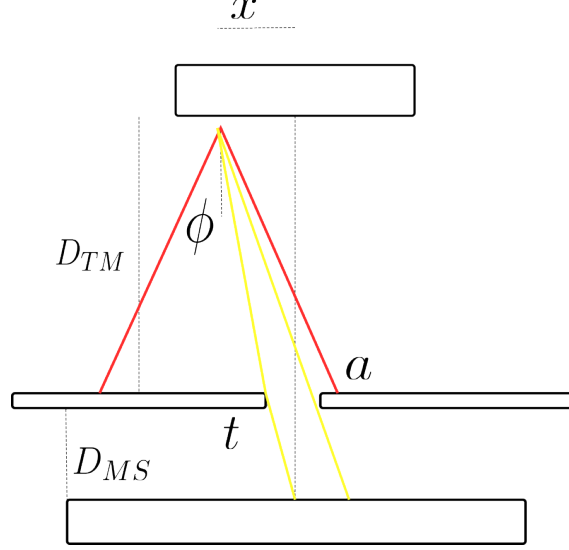
Figure 11:

relative displacement between structures of about a micron. A lift-off process which takes advantage can be easily deviced. Consider for example [33]

8 Appendix

8.1 Geometrical Blurring Effect in PLD Shadow Masking

Considering the 2D blurring for simplicity and beginning with an angular mass distribution $f(\phi)$ emerging from a point source located a distance x from the projected center of an aperture of size a. The subset of angles whit direct line of sight to the substrate are

$$\arctan(\frac{x - a/2}{D_{TM}}) < \phi < \arctan(\frac{x + a/2}{D_{TM} + t}) \tag{2}$$

and therefore the deposited mass, neglecting interaction inside the matter beam and blurring associated with surface diffusion, should be bound between

$$R \in [\frac{D}{D_{TM}}(x - a/2), \frac{D}{D_{TM} + t}(x + a/2)] \tag{3}$$

with $D = D_{TM} + D_{MS} + t$ the total distance between target and substrate.

Therefore, as $D_{TM} >> t$, one may express the geometrical blurring factor from a point-source as $B_g = \frac{D}{D_TM}$, while the defined feature is displaced with respect to the generating aperture by $d = (\frac{D}{D_{TM}} - 1)x = \frac{D_{MS}}{DTM}x$, as it also may be seem by a simple similarity between triangles.

8.2 Thickness Compensation Scheme and Blurring

Experimentally [4] one may obtain the mass distribution of a given set of deposition variables D_v, which among others may include spot size and relative position to the substrate, the light intensity profile, target material,

---

[4]This could be achieved with a dedicated profilometer, a SPM technique or by indirect methods such as mapping optical transmittance or another thickness depending property

number of pulses, atmosphere components and partial pressures, and the substrate distance, material and morphology. Let's assume that the mass distribution $M(\vec{r}, D_v)$ on the substrate is proportional to the film thickness profile $T(\vec{r}, D_v)$. By measuring such profile for a known instance of D_v, one may device a scheme to generate a particular thickness distribution on the target [5]. the problem consist on finding a set of conditions $C = D_{vi}$ such that

In the simplest case, one may keep all variables fixed but the relative position of the laser spot to the target, and assume that the total thickness profile is the sum of the contribution of equal individual pulses (indeed the ablation seems to be highly linear as long as the laser does not alter significantly the target. This is achieved by rotating the target over it's own axis to avoid ablating repetitively on the same spot).

Then our problem is to find a set of points $\vec{r}_i$ such that

$$\sum_{\vec{r}_i} T(\vec{r}_i, D_v) = \alpha \tag{4}$$

where the points $\vec{r}_i$ are constrained to the target surface and α is a certain desired thickness profile.

For most of our intended use cases, α should be a relatively uniform thickness such that $\sigma(\alpha(\vec{r}_k)) \leq \epsilon$ for $\vec{r}_k$ spanning the whole substrate surface

The problem is considerably simpler if we consider the continuum equivalent, namely to find the weight function $W(\vec{r})$ such that [6]

$$\int_{-S/2}^{S/2} W(x) T(x) dx = \alpha \tag{5}$$

8.3 Positioning Signal Processing

Due to the nature of the position feedback scheme, the desired circuit should be able to operate in noisy conditions while being able to discriminate small changes over a large signal. This suggests a auto-nulling amplifier, as one is in principle able to remove the large offset of the signal and apply a greater gain to enhance the sensitivity (which otherwise would saturate the amplifier).

While designing a decently Trans Impedance Amplifier, one is usually concerned to

References

[1] Douglas B Chrisey, Graham K Hubler, et al. *Pulsed laser deposition of thin films*. Wiley New York, 1994.

[2] Jørgen Schou. Physical aspects of the pulsed laser deposition technique: The stoichiometric transfer of material from target to film. *Applied Surface Science*, 255(10):5191–5198, 2009.

[3] Alejandro Ojeda-G-P, Max Döbeli, and Thomas Lippert. Influence of plume properties on thin film composition in pulsed laser deposition. *Advanced Materials Interfaces*, 5(18):1701062, 2018.

[4] T Venkatesan, XD Wu, A Inam, and JB Wachtman. Observation of two distinct components during pulsed laser deposition of high t c superconducting films. *Applied Physics Letters*, 52(14):1193–1195, 1988.

[5] M Peurla, P Paturi, Yu P Stepanov, Hannu Huhtinen, YY Tse, AC Bódi, J Raittila, and R Laiho. Optimization of the bazro3 concentration in ybco films prepared by pulsed laser deposition. *Superconductor Science and Technology*, 19(8):767, 2006.

---

[5]The problem is quite general, and probably the main case of practical interest is the formation on uniform layers

[6]A one dimensional analysis of the problem is first shown for simplicity

[6] Kazuhiko Tonooka, Hiroshi Bando, and Yoshihiro Aiura. Photovoltaic effect observed in transparent p–n heterojunctions based on oxide semiconductors. *Thin Solid Films*, 445(2):327–331, 2003.

[7] Arun Suresh, Praveen Gollakota, Patrick Wellenius, Anuj Dhawan, and John F Muth. Transparent, high mobility ingazno thin films deposited by pld. *Thin Solid Films*, 516(7):1326–1329, 2008.

[8] Toyanath Joshi, Tess R Senty, Robbyn Trappen, Jinling Zhou, Song Chen, Piero Ferrari, Pavel Borisov, Xueyan Song, Mikel B Holcomb, Alan D Bristow, et al. Structural and magnetic properties of epitaxial delafossite cufeo2 thin films grown by pulsed laser deposition. *Journal of Applied Physics*, 117(1):013908, 2015.

[9] C Song, KW Geng, F Zeng, XB Wang, YX Shen, F Pan, YN Xie, T Liu, HT Zhou, and Z Fan. Giant magnetic moment in an anomalous ferromagnetic insulator: Co-doped zno. *Physical Review B*, 73(2):024405, 2006.

[10] Carmen N Afonso, Rosalía Serna, Fernando Catalina, and Dionisio Bermejo. Good-quality ge films grown by excimer laser deposition. *Applied surface science*, 46(1-4):249–253, 1990.

[11] B Thestrup, B Toftmann, Jørgen Schou, B Doggett, and JG Lunney. Ion dynamics in laser ablation plumes from selected metals at 355 nm. *Applied surface science*, 197:175–180, 2002.

[12] R Dietsch, Th Holz, H Mai, C-F Meyer, R Scholz, and B Wehner. High precision large area pld of x-ray optical multilayers. *Applied surface science*, 127:451–456, 1998.

[13] O Vazquez-Mena, Leo Gross, S Xie, LG Villanueva, and Jürgen Brugger. Resistless nanofabrication by stencil lithography: A review. *Microelectronic Engineering*, 132:236–254, 2015.

[14] Oscar Vazquez-Mena, Luis Guillermo Villanueva, Veronica Savu, Katrin Sidler, Philippe Langlet, and Juergen Brugger. Analysis of the blurring in stencil lithography. *Nanotechnology*, 20(41):415303, 2009.

[15] Zoltán Rácz and Alan Seabaugh. Characterization and control of unconfined lateral diffusion under stencil masks. *Journal of Vacuum Science & Technology B: Microelectronics and Nanometer Structures Processing, Measurement, and Phenomena*, 25(3):857–861, 2007.

[16] Roli Lüthi, Reto R Schlittler, Jürgen Brugger, Peter Vettiger, Mark E Welland, and James K Gimzewski. Parallel nanodevice fabrication using a combination of shadow mask and scanning probe methods. *Applied physics letters*, 75(9):1314–1316, 1999.

[17] Gyuman Kim, Beomjoon Kim, and Jürgen Brugger. All-photoplastic microstencil with self-alignment for multiple layer shadow-mask patterning. *Sensors and Actuators A: Physical*, 107(2):132–136, 2003.

[18] Peter K Schenck, Nabil D Bassim, Makoto Otani, Hiroyuki Oguchi, and Martin L Green. Design and spectroscopic reflectometry characterization of pulsed laser deposition combinatorial libraries. *Applied surface science*, 254(3):781–784, 2007.

[19] Jingsong Wang, Young Yoo, Chen Gao, Ichiro Takeuchi, Xiaodong Sun, Hauyee Chang, X-D Xiang, and Peter G Schultz. Identification of a blue photoluminescent composite material from a combinatorial library. *Science*, 279(5357):1712–1714, 1998.

[20] Stefan Egger, Adelina Ilie, Yiton Fu, Jeffrey Chongsathien, Dae-Joon Kang, and Mark E Welland. Dynamic shadow mask technique: A universal tool for nanoscience. *Nano letters*, 5(1):15–20, 2005.

[21] Cristian-Victor Cojocaru, Riad Nechache, Catalin Harnagea, Alain Pignolet, and Federico Rosei. Nanoscale patterning of functional perovskite-type complex oxides by pulsed laser deposition through a nanostencil. *Applied surface science*, 256(15):4777–4783, 2010.

[22] E Wagner, CS Sandu, S Harada, G Benvenuti, V Savu, and P Muralt. Fabrication of complex oxide microstructures by combinatorial chemical beam vapour deposition through stencil masks. *Thin Solid Films*, 586:64–69, 2015.

[23] Nenad V Cvetkovic, Katrin Sidler, Veronica Savu, Jürgen Brugger, Dimitrios Tsamados, and Adrian M Ionescu. Three-level stencil alignment fabrication of a high-k gate stack organic thin film transistor. *Microelectronic engineering*, 88(8):2496–2499, 2011.

[24] RS Balmer, T Martin, MJ Kane, JO Maclean, TJ Whitaker, SG Ayling, PDJ Calcott, M Houlton, JP Newey, and SJ O'Mahony. Integrated laser/waveguide by shadow-masked selective area epitaxy using chemical beam epitaxy (cbe). *Journal of crystal growth*, 209(2-3):486–491, 2000.

[25] K-S Chang, MA Aronova, and I Takeuchi. Combinatorial pulsed laser deposition using a compact high-throughout thin-film deposition flange. *Applied surface science*, 223(1-3):224–228, 2004.

[26] Hideomi Koinuma and Ichiro Takeuchi. Combinatorial solid-state chemistry of inorganic materials. *Nature materials*, 3(7):429–438, 2004.

[27] Yuji Matsumoto, Makoto Murakami, Zhengwu Jin, Akira Ohtomo, Mikk Lippmaa, M Kawasaki, and Hideomi Koinuma. Combinatorial laser molecular beam epitaxy (mbe) growth of mg–zn–o alloy for band gap engineering. *Japanese Journal of Applied Physics*, 38(6A):L603, 1999.

[28] Gabriel Briceno, Hauyee Chang, Xiaodong Sun, Peter G Schultz, and X-D Xiang. A class of cobalt oxide magnetoresistance materials discovered with combinatorial synthesis. *Science*, 270(5234):273–275, 1995.

[29] JH Clark and RG Weston. An inexpensive multi-target carousel for pld systems. *Measurement Science and Technology*, 7(5):823, 1996.

[30] D Fischer, GF de La Fuente, and M Jansen. A new pulsed laser deposition technique: Scanning multi-component pulsed laser deposition method. *Review of Scientific Instruments*, 83(4).

[31] Hsien-Shun Liao, Christian Werner, Roman Slipets, Peter Emil Larsen, Ing-Shouh Hwang, Tien-Jen Chang, Hans Ulrich Danzebrink, Kuang-Yuh Huang, and En-Te Hwu. Low-cost, open-source xyz nanopositioner for high-precision analytical applications. *HardwareX*, 11:e00317, 2022.

[32] Michael Reinke, Yury Kuzminykh, and Patrik Hoffmann. Limitations of patterning thin films by shadow mask high vacuum chemical vapor deposition. *Thin Solid Films*, 563:56–61, 2014.

[33] Zoltan Racz, Jianli He, Srivatsan Srinivasan, Wei Zhao, Alan Seabaugh, Keping Han, Paul Ruchhoeft, and Jack Wolfe. Nanofabrication using nanotranslated stencil masks and lift off. *Journal of Vacuum Science & Technology B: Microelectronics and Nanometer Structures Processing, Measurement, and Phenomena*, 22(1):74–76, 2004.